IUST Iran University of Science and Technology

Iranian Journal of Electrical and Electronic Engineering

Journal Homepage: ijeee.iust.ac.ir

# Optimal Integral Sliding Mode Controller of a UAV With Considering Actuator Fault

R. Babaie* and A. F. Ehyaei*(C.A.)

**Abstract:** In this paper, using the State Dependent Riccati Equation (SDRE) method, we propose a Robust Optimal Integral Sliding Mode Controller (ROISMC) to guarantee an optimal control law for a quadrotor which has become increasingly important by virtue of its high degrees of manoeuvres ability in presence of unknown time-varying external disturbances and actuator fault. The robustness of the controller is ensured by an Integral Sliding Mode Controller (ISMC). Subsequently, based on Luenberger linear state estimator, the control algorithm is reformed and the actuator's faults are detected. Moreover, design of the controller is based on Lyapunov method which can provide the stability of all system states during the tracking of the desired trajectory. The stability of suggested algorithm is verified via the execution of sudden maneuvers subjected to forcible wind disturbance and actuator faults while performing accurate attitude and position tracking by running an extensive numerical simulation. It is comprehended that the proposed optimal robust method can achieve much better tracking capability compared with conventional sliding mode controller.

**Keywords:** Quadrotor, Integral Sliding Mode Control, SDRE, Optimal Control, Actuator's Fault.

## 1 Introduction

IN recent years, quadrotors as a type of Vertical Take-Off and Landing (VTOL) and Unmanned Aerial Vehicles (UAVs) have attracted a lot of attention, and they are increasingly being used in different areas. As a matter of fact, their advantages such as good maneuverability and small dimensions make them unique among other UAVs. Many linear methods such as PI and PID controllers [1] and LQ approach [2] have been successfully applied on quadrotors for controlling and guiding purposes. As quadrotors are nonlinear systems, several nonlinear techniques have also been suggested to control UAVs. Backstepping and feedback linearization are among the earliest techniques proposed to design robust controllers for nonlinear systems [3-5].

The quadrotor UAV is an under actuated nonlinear system with complex dynamic interaction which has six Degree-Of Freedom (DOF) while has only four rotors that able to generate four independent thrust forces. It is not facile to control all six output with only four control inputs. This will be so tough, especially if the system is in a faulty condition or exposed to the external disturbances. In order to defeat this problem, it is needed to exert capable control strategy such as the hybrid nonlinear ones to access an effective robust optimal controller. Therefore, we should resort to applying the foremost prominent tools. Using optimal control theory, control system designers can employ modern techniques for designing a control procedure to meet required specifications, performance or administrative consideration. As a result, in this paper, we guarantee the robust optimal performance of a quadrotor while addressing the trajectory tracking problem under aggressive maneuvers and actuator fault subject to rapid convergence of the system state. To accomplish this strategy, an optimization method is employed for nonlinear control procedure. We propose exerting the State Dependent Riccati Equation (SDRE) method incorporated with Integral Sliding Mode Control (ISMC) technique, called a Robust Optimal

Iranian Journal of Electrical and Electronic Engineering, 2019.
Paper first received 01 April 2018 and accepted 24 September 2018.
* The authors are with the Department of Electrical Engineering, Imam Khomeini International University, Qazvin, Iran.
E-mails: rose.babaie@gmail.com and f.ehyaei@eng.ikiu.ac.ir.
Corresponding Author: A. F. Ehyaei.

Integral Sliding Mode Control (ROISMC) strategy. In fact, the advantages of both methods are exploited.

The Sliding Mode Control method (SMC) is a well-known robust design tool for nonlinear control systems. This technique ensures insensitivity to the model errors, disturbances, and it is capable of globally stabilizing the system. Therefore, due to its robustness, SMC has been extensively used to control a quadrotor [6-8, 28]. In usual, the full response of the sliding mode control includes in two phases: the reaching phase and sliding phase. Uncertainties and perturbations may deteriorate system performance due to its sensitivity in the reaching phase. In order to properly address this problem, Integral Sliding Mode offers a solution expected to be effective on nonlinear systems however it does not include a reaching phase [9, 17]. This control method has been anxiously investigated to raise robustness of closed-loop system and decrease the influence of faulty condition or external disturbance that have destructive effects on the system performance [21-23]. Also, the authors in [20] considered the ISMC approach which incorporate with a disturbance observer to major augment the ant disturbance ability of vector control of induction motor. In the present paper, we will propose a novel ROISMC for UAV helicopter systems in the presence of actuators' fault and external disturbances by integral sliding mode controller and SDRE optimization approaches. We try to solve the optimal control problem of a UAV by applying the Riccati matrix equation method, so that the determined controller can stabilize the closed-loop system and minimize a given performance index.

The SDRE approach was first introduced by Cloutier in 1997 and is mainly about providing an optimal solution for a nonlinear dynamic system. This approach has been used as a systematic way of designing a nonlinear controller [10]. The theory of SDRE control is studied in [11], and the application of SDRE in nonlinear control problems is presented. Simple implementation and high flexibility in SDRE parameter design are among the advantages of this method. Hence, the designer can customize the parameters according to the conditions imposed by the problem. SDRE strategy puts out a principled and beneficial design of nonlinear controllers in areas such as aerospace [12], robotics technique [13,], motors [14], magnitude torque attitude control of a satellite [15], flexible cable transporter system [16] and for position and altitude control of a quadcopter [24]. Also in [25], the authors with compilation of State Dependent Riccati Equation and sliding mode method, have provided a robust optimal attitude for a nonlinear system.

On the other hand, UAV controllers require to be designed to reach the desired proficiency subject to faulty conditions. Fault tolerant controllers for quadrotors are capable of withstanding defects automatically and maintain function in case of a failure in magnetic rotors [7, 8]. In [9] the authors described a nonlinear adaptive estimation strategy which able to detect the actuator fault in a rotorcraft by using adaptive thresholds. Also in [26] authors applied a fault tolerant adaptive controller based on $\mathcal{L}1$ control algorithm to the trajectory tracking for a rotorcraft UAV in faulty condition. In these papers, the durability and the efficiency of the faulty systems are maintained by reconfiguring the controllers to take into account the actuator faults. Note that, due to the existence of complexity in controller design for UAV systems, only few research papers have considered simultaneous actuator faults and exogenous disturbances such as wind field effect. Also, to the best of authors' knowledge, no results have been reported for Integral Sliding Mode control of UAVs. Moreover, it has not been considered together with an optimal method such as SDRE in the presence of actuator fault.

In the present work, ROISMC controller is proposed to address the attitude and position control problem under aggressive maneuvers, and accurate tracking in the presence of actuator faults. It is noteworthy that there are various advantages to this method such as easy execution, smooth parameter learning to plan specification customization, principled choice of design matrices and solutions in the attendance of state's variables and control limitations. Furthermore, our control strategy in this paper is rather easy to be implemented in practical applications. Numerical simulations are provided to validate the performance of the proposed controller. The remainder of this paper is organized as follows. Section 2 introduces the dynamics of a quadrotor and its actuators based on some assumptions and simplifications. Section 3 is devoted to the problem formulation of control algorithm in two part. In the first part, the integral sliding mode control strategy is described for the stabilization of attitude and altitude and in the second part, the robust optimal controller design is presented based on SDRE method. In Section 4, the fault tolerant control technique is introduced. In Section 5, the results from numerical simulations are discussed and finally Section 6 concludes the paper with certain future development directions.

## 2 Mathematical Dynamic Model

### 2.1 Nonlinear Model of Quadrotor [19]

As is shown in Fig. 1, two basic frame are supposed to analyze dynamic model: the quadrotors earth-frame, $E = \{E_x, E_y, E_z\}$, and the body-reference frame, $B = \{B_x, B_y, B_z\}$. The position and angle vector of the UAV are denoted by $\xi = [x, y, z]^{\mathrm{T}}$ and $\eta = [\varphi, \theta, \psi]^{\mathrm{T}}$ in frame $E$, respectively.

The equation of rotational subsystem of quadrotor in body-fixed reference is defined as:

$$I\dot{\omega} + \omega \times (I\omega) = \tau + \delta_{\tau} \tag{1}$$

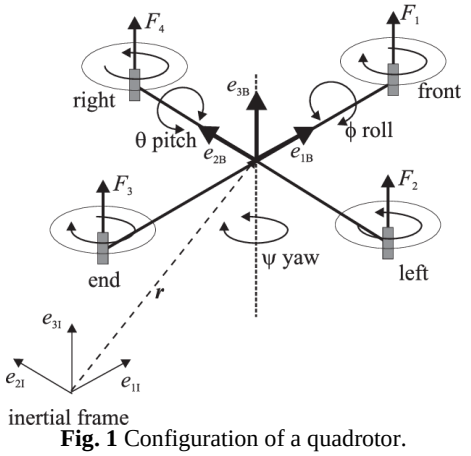


**Fig. 1** Configuration of a quadrotor.

where, $\tau = [\tau_\varphi\ \tau_\theta\ \tau_\psi]^T$ denotes the rotation torques of propellers, $I$ = diag$\{I_x, I_y, I_z\}$ is the diagonal inertia matrix respect to the $E$ reference, $\omega = [p\ q\ r]^T$ shows the angular velocity and $\delta_\tau = [\delta_\varphi, \delta_\theta, \delta_\psi]^T$ refers to the vector of external disturbances. Also, the equation of rotational subsystem of quadrotor in body-fixed reference is described as:

$$m\dot{V} + \omega \times (mV) = F + \delta_F \tag{2}$$

where $V = [V_x\ V_y\ V_z]^T$ is the quadrotor linear velocity, $F = [F_x\ F_y\ F_z]^T$ denotes the thrust forces which produced by rotors, $\delta_F = [\delta_x, \delta_y, \delta_z]^T$ is the vector of external disturbances and $m$ represents the mass of quadrotor. Using (1) and (2), the full quadrotor dynamic model is described as follows:

$$\begin{cases} \ddot{x} = (\cos\varphi\sin\theta\cos\psi + \sin\varphi\sin\psi)\dfrac{1}{m}u_1 + \delta_x \\ \ddot{y} = (\cos\varphi\sin\theta\sin\psi - \sin\varphi\sin\psi)\dfrac{1}{m}u_1 + \delta_y \\ \ddot{z} = -g + (\cos\varphi\cos\theta)\dfrac{l}{m}u_1 + \delta_z \end{cases}$$

$$\begin{cases} \ddot{\varphi} = \dot{\theta}\dot{\psi}\left(\dfrac{Iy - Iz}{Ix}\right) - \dfrac{jr}{Ix}\dot{\theta}\Omega + \dfrac{l}{I_x}u_2 + \delta_\varphi \\ \ddot{\theta} = \dot{\varphi}\dot{\psi}\left(\dfrac{Iz - Ix}{Iy}\right) - \dfrac{jr}{Ix}\dot{\varphi}\Omega + \dfrac{l}{y}u_3 + \delta_\vartheta \\ \ddot{\psi} = \dot{\varphi}\dot{\theta}\left(\dfrac{Ix - Iy}{Iz}\right) + \dfrac{l}{Iz}u_4 + \delta_\psi \end{cases} \tag{3}$$

The input $u_1$ denotes the total generated translational thrust forces; while the inputs $u_2$, $u_3$, and $u_4$ are respected to the rotational thrust force of the quadrotor, $jr$ describes the inertia of the $Z$ axis and $\Omega$ expresses the overall residual propeller angular speed. where:

$$\begin{cases} U_1 = b\left(\Omega_4^2 - \Omega_3^2\right) = F_4 - F_3 \\ U_2 = lb\left(\Omega_2^2 - \Omega_1^2\right) = F_2 - F_1 \end{cases}$$

$$\begin{cases} U_3 = lb\left(\Omega_1^2 + \Omega_2^2 - \Omega_3^2 - \Omega_4^2\right) = F_1 + F_2 - F_3 - F_4 \\ U_4 = d\left(\Omega_1^2 + \Omega_2^2 + \Omega_3^2 + \Omega_4^2\right) = F_1 + F_2 + F_3 + F_4 \\ \Omega = -\Omega_1 - \Omega_2 + \Omega_3 + \Omega_4 \end{cases} \tag{4}$$

Also $k$ and $b$ represent the thrust and drag coefficient. The system (3) can be represented in a state-space form $\dot{x} = f(x, U)$ by considering $x_i = [x_1, \ldots, x_{12}]$, $i \in (1, 12)$ which shows the state variables as follows:

$x_1 = \varphi$, $x_2 = \dot{x}_1 = \dot{\varphi}$, $x_3 = \theta$, $x_4 = \dot{x}_3 = \dot{\theta}$, $x_5 = \psi$, $x_6 = \dot{x}_5 = \dot{\psi}$, $x_7 = x$, $x_8 = \dot{x}_7 = \dot{x}$, $x_9 = y$, $x_{10} = \dot{x}_9 = \dot{y}$, $x_{11} = z$, $x_{12} = \dot{x}_{11} = \dot{z}$.

$$f(x,U) = \begin{pmatrix} x_2 \\ x_4x_6a_1 + x_4x_2\Omega + b_1u_2 + \delta_\varphi \\ x_4 \\ x_2x_6a_3 + x_2a_4\Omega + b_2u_3 + \delta_\theta \\ x_6 \\ x_4x_2a_5 + b_3u_4 + \delta_\psi \\ x_8 \\ (\cos x_1 \sin x_3 \cos x_5 + \sin x_1 \sin x_5)\dfrac{1}{m}u_1 + \delta_x \\ x_{10} \\ (\cos x_1 \sin x_3 \sin x_5 - \sin x_1 \sin x_5)\dfrac{1}{m}u_1 + \delta_y \\ x_{12} \\ -g + (\cos x_1 \ \cos x_3)\dfrac{1}{m}u_1 + \delta_z \end{pmatrix} \tag{5}$$

$a_1 = (I_y – I_z)/I_x$, $a_2 = –jr/I_x$, $a_3 = (I_z – I_x)/I_y$, $a_4 = jr/I_y$, $a_5 = (I_x – I_y)/I_z$, $b_1 = l/I_x$, $b_2 = l/I_y$, $b_3 = l/I_z$ (6)

### 2.2 Dynamics of Actuators

Each propeller of quadrotor generates a thrust force which can be modeled as a first order system;

$$F_i = k\frac{w_0}{s + w_0}u_i \tag{7}$$

where, $w_0$ shows the bandwidth of actuator and $k$ is a positive and non-zero gain. The variable $v_i$ shows the dynamics of actuator, which is described as follows:

$$v_i = \frac{w_0}{s + w_0}u_i \tag{8}$$

**Assumption 1**. It is assumed that the roll, pitch and yaw angle satisfy the conditions $|\varphi(t)| < \pi/2$, $|\theta(t)| < \pi/2$, and $|\psi| < \pi$ for $t \geq 0$.

**Assumption 2.** In general, the parameter disturbance $\delta = [\delta_x, \delta_y, \delta_z, \delta_\varphi, \delta_\theta, \delta_\psi]^T$ is assumed bounded uncertainty, i.e. $|\delta| \leq \gamma$ where $\gamma$ is positive constant. This assumption is also authentic for matched and mismatched uncertainties when there is knowledge about the uncertain terms based on systems states.

## 3 Problem Formation of the Robust Optimal Controller Synthesis

In this section, our main purpose is to develop an optimal robust tracking controller for the system (3) based on Integral sliding mode technique (ISMC) and state-dependent Riccati equation (SDRE) theory. This controller can ensure the safety performance and the asymptotic stability of the translational and rotational motions of UAV system. For better illustrating of the proposed controller, we have done design procedure in three steps. In the first step, the integral sliding mode controller is introduced and subsequently the SDRE strategy will be presented in the second part. Finally, in the last part, control law of the algorithm can be extracted by combining the ISMC approach with SDRE strategy in order to generate a robust and optimal solution for this non-linear dynamic control scheme. One of the more prominent aspects of this control approach is its robustness against external disturbances and faulty condition. Due to absence of optimization in Integral sliding mode strategy, in this research, a robust and optimal method is described by introducing the SDRE in sliding surface design. Moreover, by compositing the SDRE theory in the design of sliding surface of ISMC, the suggested method is capable to access finite-time control conditions. Also, note that the same initial constraints are imposed to both of the designed controller and conventional SMC in order to obtain the effective comparability in simulations.

### 3.1 Integral Sliding Mode Control

Sliding mode is a powerful controlling method used in design and implementation of different systems from several aspects. In this section, a sliding mode is designed via a nonlinear integral sliding surface to remove chattering and provide good speed response. The following system with uncertain nonlinear dynamic equation is considered:

$$\dot{x}(t) = f(x) + g(x)u(t) + \delta(x,t),\ Y = Cx(t) \tag{9}$$

where $u(t) \in R^m$ is the control vector, $f(x) \in c^q$ and $g(x) \in c^q$ with $q \geq 1$ represent nonlinear functions of $x$ respectively. $\delta(x, t)$ is an indefinite function which describe existence of external disturbance. The nonlinear integral sliding function is expressed as follows [13]:

$$\sigma_{ISMC}(t) = -T\left(x_i(t) - x_i(0)\right) + \Upsilon\int_0^t (f + gN)x(s)d(s) \tag{10}$$

where $\Upsilon \in R^{n\times n}$ is the matrix selected to be full rank, $T \in R^{n\times m}$ and $N \in R^{n\times m}$ are non-variable matrices. The matrix $N$ is chosen such that the matrix $f + gN$ is Hurwitz, and $T$ is selected such that $Tg = I_m$ is nonsingular and can be proved that $\|I–g(Tg)^{-1}T\| \geq 1$ for any $T$. When $\sigma_{ISMC}(t) = 0$ the stability result for uncertain switched system is given. It is evident from (10) that the sliding surface is designed in an integral form, and it depends on the initial condition $x_i(0)$. So the sliding function expressed in (10) can be chosen as follows [18]:

$$T = \Upsilon C R_d^{-1} \tag{11}$$

where $R_d \in R^{n\times m}$ is a matrix with eigenvalues which are selected to be equal to the poles of close loop system. When $x_i$ erupts in the sliding surface, we have $\sigma_{ISMC}(t) = 0$, and the time differentiating of the sliding function can be described as;

$$\begin{aligned}\dot{\sigma}_{ISMC}(t) &= \\ &= -T\dot{x}(t) + \Upsilon(f + gN) \\ &= -T\left(f(x) + g(x)u(t) + \delta(x,t)\right) \\ &\quad + \Upsilon\left(f(x) + g(x)N\right)\end{aligned} \tag{12}$$

Also, the control function is represented as follows;

$$u(t) = u_n + u_l \tag{13}$$

Then, using (12), the equivalent control $u_{equ\text{-}ISMC}$ can be earned by solving $\dot{\sigma}_{ISMC}(t) = 0$:

$$\begin{aligned}u_{equ-ISMC} &= \\ &= g(x)^{-1}\left\{f(x) + \delta(x,t)\right\} \\ &= \left(Tg(x)\right)^{-1}\Upsilon f(x) + T^{-1}\Upsilon\end{aligned} \tag{14}$$

The nonlinear sliding mode control law $u_n$ is normally the equivalent control of system (9) expressed as:

$$\begin{aligned}u_n = g(x)^{-1}&\left\{f(x)\left(1 + \left(CR_d^{-1}\right)^{-1}\right) + \delta(x,t)\right\} \\ &+ \left(CR_d^{-1}\right)^{-1}N\end{aligned} \tag{15}$$

A necessary condition to be ensured of sliding action in finite time in the presence of ambiguity and external disturbances is described as [18,9];

$$\sigma_{ISMC}^T(t)\dot{\sigma}_{ISMC}(t) \leq -\Lambda\left\|\sigma_{ISMC}(t)\right\| \tag{16}$$

where $\Lambda$ demonstrates a positive scalar matrix. The Eq. (13) shows that $\Lambda$-reachability condition is satisfied, which ensures the existence of an sliding motion on the sliding surface $\sigma(t)$. A Lyapunov function can be written as $V = \sum\frac{1}{2}\sigma^T\sigma$. So according to (16), the sufficient condition for the stability of the system is defined by;

$$\dot{V}(t) = -\Lambda\left|\sigma(t)\right| = -\Lambda\sqrt{2V(t)} \tag{17}$$

By integrating both sides of the Eq. (16) yields

$$\sqrt{2V(t)} - \sqrt{2V(0)} \le -\Lambda t \tag{18}$$

which denotes $V(t) \equiv 0$ in less than $\frac{\sqrt{2V(0)}}{\Lambda}$ units of time.

### 3.2 SDRE Controller Structure Regulation

The SDRE feedback control exerts extended linearization strategy to the formulation of nonlinear optimal problem for the input-affine system (9) as a linear control combination approach (LQR).By considering system (9), let $u = u(t)$ where $u$ should be determined such that it minimizes the following performance index [19]:

$$J = \frac{1}{2}\int_0^\infty \left[x^T(t)Q(x)x(t) + u^T R(x)u\right]dt \tag{19}$$

$Q(x) \in c^q$, $R(x) \in c^q$ (for $q > 1$) are the weighting matrices which are related to the state variable $x$. Also, $R(x)$ is respected to be a positive definite matrix, while $Q(x)$ is a semi-positive definite matrix. The mathematical equation of the system (9) can be rewritten as follows to solve the problem by SDRE method,

$$\dot{x}(t) = f(x)x(t) + g(x)u(t) + \delta(x,t) \tag{20}$$

It is also assumed that $\|\delta(x, t)\| \le \gamma_0 + \gamma_1\|x(t)\|$, for positive constants $\gamma_0$ and $\gamma_1$. The optimal state feedback control law can easily be proved to be as:

$$u(x) = -R^{-1}(x)g^T(x)P(x)x(t) \tag{21}$$

where $P(x)$ is a positive, symmetric and unique matrix. In the next step by solving the algebraic Riccati equation, the control law can be determined as follows:

$$f^T(x)P(x) + P(x)f(x) + Q(x) - P(x)g(x)R^{-1}(x)g^T(x)P(x) = 0 \tag{22}$$

Then, by considering the uncertain system (20), the optimal sliding surface is selected as (23) to develop the optimal control law which is related to integral sliding mode:

$$\begin{aligned}\sigma_{opt}(t, x(t)) &= H(x)\left[x(t) - x(0)\right] \\ &- H(x)\int_0^t \left[f(x)x(t) - g(x)R^{-1}g^T(x)P(x)\right]x(\tau)d\tau\end{aligned} \tag{23}$$

where $H(x) \in R^{m\times n}$ and $\{H(x), g(x)\}$ is nonsingular. Eq. (23) clearly indicates that $\sigma_{opt}(0, x(0)) = 0$ when $t = 0$; thus, the system always starts at the predefined sliding surface. Now, in case of $\dot{\sigma}_{opt} = 0$, equivalent control law is obtained as follows:

$$\begin{aligned}u_{equ-optimal} &= \\ &-\left[H(x)g(x)\right]^{-1}\left[H(x)\delta(x,t)\right. \\ &\left. + H(x)g(x)R^{-1}g^T(x)P(x)x(\tau)\right]\end{aligned} \tag{24}$$

The nominal equivalent control which is related to the linear part of control function, is gained by SDRE according to Eqs. (23) and (24) as follows:

$$\begin{aligned}u_l = &\left[H(x)g(x)\right]^{-1} \times \\ &\left[k + \gamma_0 H(x)g(x) + \gamma_1 H(x)g(x)x(\tau)\right] \times \\ &\operatorname{sgn}(\sigma_{opt})\end{aligned} \tag{25}$$

### 3.3 Robust Optimal Control Law

The control law based on (15) and (25) can be written as follows;

$$\begin{aligned}u = &g(x)^{-1}\left\{f(x)\left(1 + \left(CR_d^{-1}\right)^{-1}\right) + \delta(x,t) - \dot{x}_i(0)\right\} \\ &+ \left(CR_d^{-1}\right)^{-1} N + \left[H(x)g(x)\right]^{-1} \times \\ &\left[k + \gamma_0\|H(x)g(x)\| + \gamma_1\|H(x)g(x)\|\|x(\tau)\|\right]\operatorname{sgn}(\sigma_{opt})\end{aligned} \tag{26}$$

In (26), k > 0 is an appropriate constant value, and $\operatorname{sgn}(\sigma_{opt}) = [\operatorname{sgn}(\sigma_{ISMC,1}), \ldots, \operatorname{sgn}(\sigma_{ISMC,m})]^T$.

An adequate condition for constancy of proposed control law is $\dot{V} = \sigma_{opt}^T\dot{\sigma}_{opt} < 0$. However, with regard to the described Lyapunov function, we are able to prove the asymptotically stability of it:

$$\begin{aligned}\dot{V} = &-k\left\|\sigma_{opt}\right\|_1 + \sigma_{opt}^T\dot{H}(x)g\tilde{\delta}(x,t) \\ &-\left[\gamma_0\left\|H(x)g(x)\right\| + \gamma_1\left\|H(x)g(x)\right\|\|x\|\right]\left\|\sigma_{opt}\right\|_1\end{aligned} \tag{27}$$

Therefore:

$$\begin{aligned}\dot{V} \le &-k\left\|\sigma_{opt}\right\|_1 + \left\|H(x)g(x)\right\|\left\|\sigma_{opt}\right\|(\gamma_0 + \gamma_1)\|x\| \\ &-\left[\left\|\sigma_{opt}\right\| - \left\|\sigma_{opt}\right\|_1\right]\end{aligned} \tag{28}$$

where $\|\sigma_{opt}\|_1$ represents 1-norm, and as $\|\sigma_{opt}\|_1 \ge \|\sigma_{opt}\|$ the following result can be achieved;

$$\dot{V} = \sigma_{opt}^T\dot{\sigma}_{opt} \le k\left\|\sigma_{opt}\right\| < 0 \quad \text{for} \left\|\sigma_{opt}\right\| \ne 0 \tag{29}$$

Now, from (20), the optimized switching surface are chosen as:

$$\sigma_{opt} = \left[\sigma_{ISMC,1}, \ldots, \sigma_{ISMC,m}\right]^T \tag{30}$$

After choosing switching surface variables, to earn variable $H(x)$, the following relations are expressed:

$$ME = \left[ME_1, ME_2, \ldots, ME_{12}\right]^T$$

$$\left[x(t)-x(0)\right]^{\mathrm{T}}-\int_0^t\left[f(x)x-g(x)R^{-1}g^{\mathrm{T}}(x)P(x)\right]x(\tau)d\tau \quad (31)$$

Finally the variable $H(x)$ defined according to (32)

$$H(x).ME=\sigma_{opt} \quad (32)$$

By considering (31), it is obvious that $H(x)$ is not unique matrix and should be used to the non-singularity condition of $\{H(x), g(x)\}$. So $H(x)$ is selected as follows:

$$H(x)=\begin{pmatrix}
0 & \left|\frac{\sigma_{opt}/n_1}{ME_2}\right| & 0 & 0 & 0 & 0 & 0 & 0 & 0 & 0 & 0 & 0\\
0 & 0 & 0 & \left|\frac{\sigma_{opt}/n_2}{ME_4}\right| & 0 & 0 & 0 & 0 & 0 & 0 & 0 & 0\\
0 & 0 & 0 & 0 & 0 & \left|\frac{\sigma_{opt}/n_3}{ME_6}\right| & 0 & 0 & 0 & 0 & 0 & 0\\
0 & 0 & 0 & 0 & 0 & 0 & 0 & \left|\frac{\sigma_{opt}/n_4}{ME_8}\right| & 0 & 0 & 0 & 0\\
0 & 0 & 0 & 0 & 0 & 0 & 0 & 0 & 0 & \left|\frac{\sigma_{opt}/n_5}{ME_{10}}\right| & 0 & 0\\
0 & 0 & 0 & 0 & 0 & 0 & 0 & 0 & 0 & 0 & 0 & \left|\frac{\sigma_{opt}/n_6}{ME_{12}}\right|
\end{pmatrix} \quad (33)$$

where $n_1$, …, $n_6$ are arbitrary non zero constants. The $f(x)$ and $g(x)$ matrices, are regulated according to (34);

$$f(x)=\begin{pmatrix}
0 & 1 & 0 & 0 & 0 & 0 & 0 & 0 & 0 & 0 & 0 & 0\\
0 & 0 & 0 & a_2\Omega & 0 & x_4a_1 & 0 & 0 & 0 & 0 & 0 & 0\\
0 & 0 & a_2\Omega & 0 & 0 & 0 & x_4a_1 & 0 & 0 & 0 & 0 & 0\\
0 & 0 & 0 & x_6a_5 & 0 & 0 & 1 & 0 & 0 & 0 & 0 & 0\\
0 & 0 & 0 & 0 & 0 & 0 & 0 & 1 & 0 & 0 & 0 & 0\\
\frac{-g}{x_7} & 0 & 0 & 0 & 0 & 0 & 0 & 0 & 0 & 0 & 0 & 0\\
0 & 0 & 0 & 0 & 0 & 0 & 0 & 0 & 0 & 1 & 0 & 0\\
0 & 0 & 0 & 0 & 0 & 0 & 0 & 0 & 0 & 0 & 0 & 0\\
0 & 0 & 0 & 0 & 0 & 0 & 0 & 0 & 0 & 0 & 0 & 1\\
0 & 0 & 0 & 0 & 0 & 0 & 0 & 0 & 0 & 0 & 0 & 0
\end{pmatrix},$$

$$g(x)=\begin{pmatrix}
0 & 0 & 0 & 0 & 0 & 0\\
0 & b_1 & 0 & 0 & 0 & 0\\
0 & 0 & 0 & 0 & 0 & 0\\
0 & 0 & b_2 & 0 & 0 & 0\\
0 & 0 & 0 & 0 & 0 & 0\\
0 & 0 & 0 & b_3 & 0 & 0\\
0 & 0 & 0 & 0 & 0 & 0\\
\frac{cosx_1cosx_3}{m} & 0 & 0 & 0 & 0 & 0\\
0 & 0 & 0 & 0 & 0 & 0\\
0 & 0 & 0 & 0 & \frac{1}{m}U_1 & 0\\
0 & 0 & 0 & 0 & 0 & 0\\
0 & 0 & 0 & 0 & 0 & \frac{1}{m}U_1
\end{pmatrix} \quad (34)$$

Also, one of important parts in designing a SDRE controller is the selection of weighting matrices $Q(x)$ and $R(x)$ For better results, these matrices should be state-dependent. Therefore matrices $Q(x)$ and $R(x)$, are chosen as follows:

$$Q(x)=\begin{pmatrix}
1 & 0 & 0 & 0 & 0 & 0 & 0 & 0 & 0 & 0 & 0 & 0\\
0 & 1 & 0 & 0 & 0 & 0 & 0 & 0 & 0 & 0 & 0 & 0\\
0 & 0 & 1 & 0 & 0 & 0 & 0 & 0 & 0 & 0 & 0 & 0\\
0 & 0 & 0 & 1 & 0 & 0 & 0 & 0 & 0 & 0 & 0 & 0\\
0 & 0 & 0 & 0 & 1 & 0 & 0 & 0 & 0 & 0 & 0 & 0\\
0 & 0 & 0 & 0 & 0 & 1 & 0 & 0 & 0 & 0 & 0 & 0\\
0 & 0 & 0 & 0 & 0 & 0 & \frac{0.3}{|x_7|} & 0 & 0 & 0 & 0 & 0\\
0 & 0 & 0 & 0 & 0 & 0 & 0 & 0.005 & 0 & 0 & 0 & 0\\
0 & 0 & 0 & 0 & 0 & 0 & 0 & 0 & \frac{0.3}{|x_9|} & 0 & 0 & 0\\
0 & 0 & 0 & 0 & 0 & 0 & 0 & 0 & 0 & 0.005 & 0 & 0\\
0 & 0 & 0 & 0 & 0 & 0 & 0 & 0 & 0 & 0 & \frac{0.3}{|x_{11}|} & 0\\
0 & 0 & 0 & 0 & 0 & 0 & 0 & 0 & 0 & 0 & 0 & 0.005
\end{pmatrix},$$

$$R(x)=\begin{pmatrix}
0.008 & 0 & 0 & 0 & 0 & 0\\
0 & 0.2|x_7^2| & 0 & 0 & 0 & 0\\
0 & 0 & 0.008 & 0 & 0 & 0\\
0 & 0 & 0 & 0.2|x_9^2| & 0 & 0\\
0 & 0 & 0 & 0.008 & 0 & 0\\
0 & 0 & 0 & 0 & 0 & 0.4|x_{11}^2|
\end{pmatrix} \quad (35)$$

## 4 Effects of Actuator Faults

In this section in order to show that the designed robust optimal controller is thoroughly impressive under destructive effects, in addition to the presence of external disturbances, the system is exposed to actuator restrictions. One of the most important sources of fault generation is actuator's faults which we discuss it on the performance of system. It is very possible that one or more rotors of UAV in a long time duty loses its efficiency. In fact, in this circumstances, the rotors are working, but cannot generate desired influence. It can be a proper strategy to estimate the output of rotors.

To this end, we use a linear estimation method called Luenberger linear state estimator that linearizes the quadrotor system around its equilibrium point, and finally estimates the faults of actuators in the system as the state variables of the system [27]. After estimating, the fault detection unit measures the amounts of difference between outputs of the rotors with nominal values to detect the faults have accrued in the UAV system. In this faulty condition, the control algorithm attempts to reform the system for fault tolerant control.

Therefore, in this step we define modification transform equation based on Eq. (4),in order to regulate trust forces $F_i$ without any changing in control signal $u_i$ as follows:

$$\begin{cases} \Omega_1^2 = \frac{1}{4b}u_1 - \frac{1}{2bl}u_2 + \frac{1}{4d}u_4 \\ \Omega_2^2 = \frac{1}{4b}u_1 + \frac{1}{2bl}u_3 - \frac{1}{4d}u_4 \\ \Omega_1^2 = \frac{1}{4b}u_1 + \frac{1}{2bl}u_2 + \frac{1}{4d}u_4 \\ \Omega_1^2 = \frac{1}{4b}u_1 - \frac{1}{2bl}u_3 - \frac{1}{4d}u_4 \end{cases} \quad (36)$$

According to (4), the fault in each rotor is modeled as a bias multiplied by the forces:

*If accrued fault is in Motor #1:*

$$\begin{cases} u_1 = F_4 - F_3 \\ u_2 = +F_2 \\ u_3 = -F_2 - F_3 + F_4 \\ u_4 = F_2 + F_3 + F_4 \end{cases} \quad (37)$$

*If accrued fault is in Motor #2:*

$$\begin{cases} u_1 = F_4 - F_3 \\ u_2 = -F_1 \\ u_3 = F_1 - F_3 + F_4 \\ u_4 = F_1 + F_3 + F_4 \end{cases} \quad (38)$$

*If accrued fault is in Motor #3:*

$$\begin{cases} u_1 = F_4 \\ u_2 = F_2 - F_1 \\ u_3 = F_1 + F_2 - F_4 \\ u_4 = F_1 + F_2 + F_4 \end{cases} \quad (39)$$

*If accrued fault is in Motor #4:*

$$\begin{cases} u_1 = -F_3 \\ u_2 = F_2 - F_1 \\ u_3 = F_1 + F_2 - F_3 \\ u_4 = F_1 + F_2 + F_3 \end{cases} \quad (40)$$

The main aim of a fault tolerant controller is to land the quadrotor horizontally and safely when an actuator fault happens in each rotor. Another factor that makes the control algorithm different in the faulty mode and the normal mode is that when each motor of the quadrotor is faulty, it may not provide sufficient thrust for other control signals, so that the faulty rotor does not take part in the control of its angle or height. For example, according to (4), in the normal mode, signal $u_1$ which controls the roll angle is equal to the difference of trust forces of the motors 3 and 4. But note that if we consider failure as a reduction of the performance of motor 3, it is probable that it cannot provide sufficient trust for signal $u_1$. To overcome this problem, we omit the effect of motor 3 in signal $u_1$ and put out this signal only with the motor 4. Finally, the fault tolerant algorithm of controller reformation based on the relation between outputs of the rotors in (36) can be described as:

*If accrued fault is in Motor #1:*

$$\begin{pmatrix} F_1 \\ F_2 \\ F_3 \\ F_4 \end{pmatrix} = \begin{pmatrix} \frac{1}{4}u_4 \\ u_2 + \frac{1}{4}u_4 \\ -\frac{1}{2}u_1 + \frac{1}{4}u_4 \\ \frac{1}{2}u_1 + \frac{1}{4}u_4 \end{pmatrix} \quad (41)$$

*If accrued fault is in Motor #2:*

$$\begin{pmatrix} F_1 \\ F_2 \\ F_3 \\ F_4 \end{pmatrix} = \begin{pmatrix} -u_1 + \frac{1}{4}u_4 \\ \frac{1}{4}u_4 \\ -\frac{1}{2}u_1 + \frac{1}{4}u_4 \\ \frac{1}{2}u_1 + \frac{1}{4}u_4 \end{pmatrix} \quad (42)$$

*If accrued fault is in Motor #3:*

$$\begin{pmatrix} F_1 \\ F_2 \\ F_3 \\ F_4 \end{pmatrix} = \begin{pmatrix} -\frac{1}{2}u_2 + \frac{1}{4}u_4 \\ \frac{1}{2}u_2 + \frac{1}{4}u_4 \\ \frac{1}{4}u_4 \\ u_1 + \frac{1}{4}u_4 \end{pmatrix} \quad (43)$$

*If accrued fault is in Motor #4:*

$$\begin{pmatrix} F_1 \\ F_2 \\ F_3 \\ F_4 \end{pmatrix} = \begin{pmatrix} -\frac{1}{2}u_2 + \frac{1}{4}u_4 \\ \frac{1}{2}u_2 + \frac{1}{4}u_4 \\ -u_1 + \frac{1}{4}u_4 \\ \frac{1}{4}u_4 \end{pmatrix} \quad (44)$$

Finally, in simulation section we will demonstrate that

the designed controller in section.3 has achieved to accurate and acceptable results in spite of the occurrence of faults in the form of partial loss of rotor effectiveness.

## 5 Simulation Results

To compare the effectiveness of proposed controller on system performance and the reduced tracking errors, three cases are considered. The first simulation is considered in order to point to point path planning from different initial conditions. In this case, the quadrotor is subjected to the unknown external wind disturbances with a fixed velocity. The second simulation considers aggressive maneuvers under unknown time-varying wind disturbances, to track a predefined sinusoidal trajectory. Finally, the third case is to carry out aggressive maneuver under time varying wind disturbances to track square waveform reference trajectories. The parameters for simulation of a sample quadrotor model are set as $m$ = 1.77 kg, $d$ = 0.225 m, $I_x$ = $2.16\times10^{-3}$ kg.m$^2$, $I_y$ = $2.16\times10^{-3}$ kg.m$^2$, $I_z$ = $0.33\times10^{-3}$ kg.m$^2$, $g$ = 9.81 m/s$^2$, $J_r$ = $3.357\times10^{-5}$ kg.m$^2$, $b$ = $2.98\times10^{-6}$, $l$ = 0.42 m. Also the parameters of proposed controller are selected as follows;

$$T = \begin{bmatrix} -0.434 & -0.656 & -0.232 & -0.121 & 0.765 & 0.876 \\ -0.614 & -0.751 & -0.232 & 0.121 & 0.765 & 0.876 \end{bmatrix}$$

$$\Lambda = \begin{bmatrix} 0.0211 & 0.0639 & 0.765 & 0.0.221 & 0.921 & 0.994 \\ 0.0112 & 0.0156 & 0.876 & 0.164 & 0.665 & 0.0212 \end{bmatrix}$$

$$\left[n_1, n_2, n_3, n_4, n_5, n_6\right]^T = \left[0.0234, 0.087, 0.0766, 0.0349, 0.0423, 0.0265\right]^T$$

Also, the effect of unknown time varying wind disturbance, is considered as follows:

$$\delta(x,t) = \begin{bmatrix} \delta_1(t) \\ \delta_2(t) \\ \delta_3(t) \end{bmatrix} = \begin{bmatrix} 0.5\sin\left(\frac{\pi(t-20)}{10}\right) + 0.02\sin\left(\frac{\pi(t-20)}{5}\right) \\ 0.5\sin\left(\frac{\pi(t-30)}{10}\right) + 0.02\sin\left(\frac{\pi(t-30)}{5}\right) \\ 0.5\sin\left(\frac{\pi(t-40)}{10}\right) + 0.02\sin\left(\frac{\pi(t-40)}{5}\right) \end{bmatrix} m/s^2 \quad (45)$$

Note that, in all simulation cases, the faulty conditions are quite similar. The actuator fault scenario considered here assumes that the first rotor undergoes a 25% loss of its trust force at $t$ = 1.8 s, and third rotor undergoes a 35% loss of its trust force at $t$ = 1.8 s, while the second and forth rotors produce 100% of maximum values of their trust forces. The Fig. 2 demonstrates the fault detection outputs.

### 5.1 Point to Point Path Planning Under Wind Gusts With a Fixed Velocity

In this section, the quadrotor is subjected to the unknown external wind disturbances with a fixed velocity of 3.6 m/s. For the first simulation, the initial values for the rotational subsystem are chosen as $[\varphi, \theta, \psi] = [\pi/4, \pi/4, \pi/4]^T$, the desired angles as $[\varphi, \theta, \psi] = [0, 0, 0]^T$, the initial values for translational subsystem as $[x, y, z] = [0.1, 0.01, 0.1]^T$ and the desired position set as $[x, y, z] = [2, 2, 2]^T$. The position and attitude angle response of the system in the presence of wind field and actuator fault are shown in Figs. 3 and 4. For the attitude angle the controller stabilized it at zero in a short period of time. Pitch angle $\theta$ is stabilized at 0.027 rad, roll angle $\varphi$ at 0.011 rad, and yaw angle $\psi$ at 0.013 rad. We can see that with the wind field effects, the oscillation of attitude angle and the settling time in ROISMC method are lower in comparison to SMC method. Using the ROISMC, a smooth reference tracking is performed. We observe that the quadrotor reaches to the position value rapidly. In fact, it is settled down at the desired value in less than 2 seconds. Although, in the beginning of the tracking where the vehicle is far from the trajectory there exists a significant error. This is due to the different actual position and reference position in the beginning of motion. Then, the controller tries to decrease the error of tracking in next times during the simulation. Fig. 5 shows the stability of rotor speed of a quadrotor during hovering. One can see that the range of control input is greatly decreased which confirms the other advantage of the SDRE approach. Trajectory of the quadrotor in 3D space is also shown in Fig. 6.

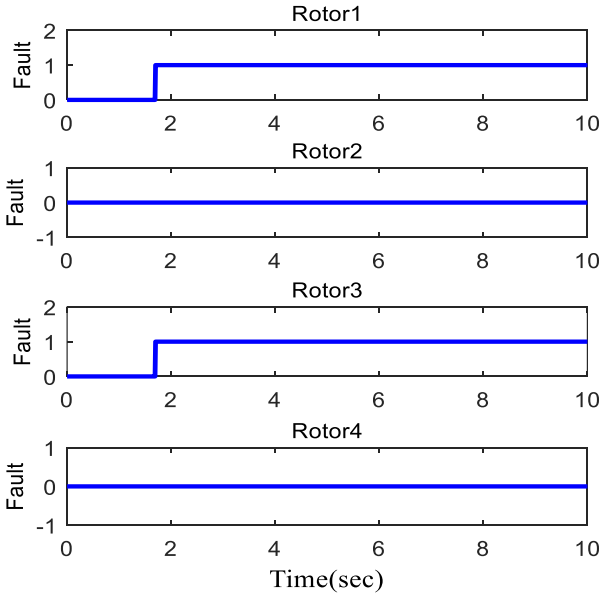


**Fig. 2** The outputs of fault detection.

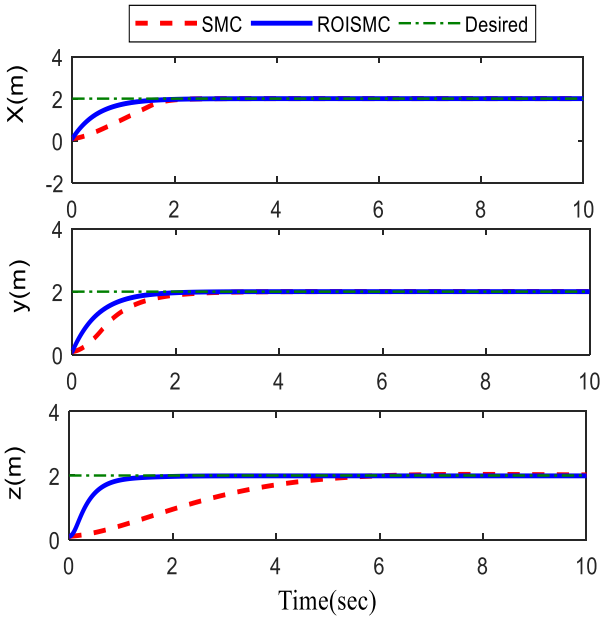


**Fig. 3** Tracking results of position ($x$, $y$, $z$).

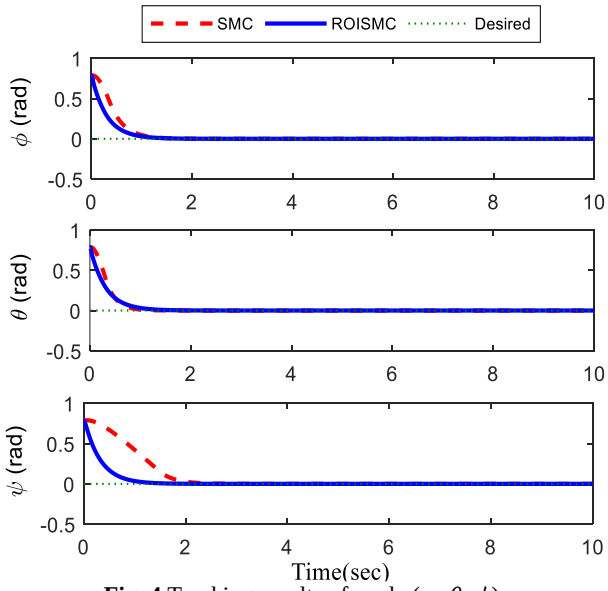


**Fig. 4** Tracking results of angle ($\varphi$, $\theta$, $\psi$).

Another finding is that, with the increase of wind speed, the oscillation of attitude angle and the time to settle the system down are become greater. A comparison of the mean square error (MSE) for both SMC and ROISMC control is being presented in Fig. 7.

In most cases, given the large sampling period $1/T_s$ = 0.001 s, the ROISMC-controlled system has superior response, and still outperforms compared with the SMC control scheme when the sampling period decreases ($1/T_s$ = 0.01 s).

### 5.2 Aggressive Maneuvers in Predefined Sinusoidal Trajectory Tracking Under Time-Varying Wind Disturbances

In order to investigate the efficiency of the proposed

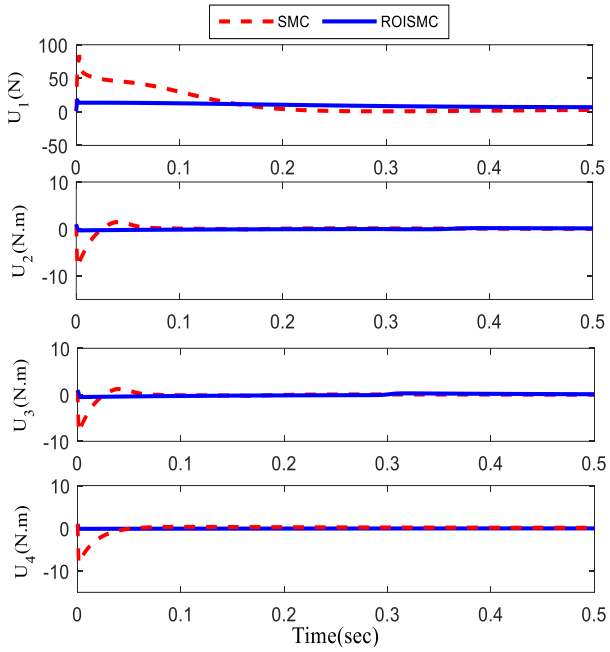


**Fig. 5** The output of the actuators.

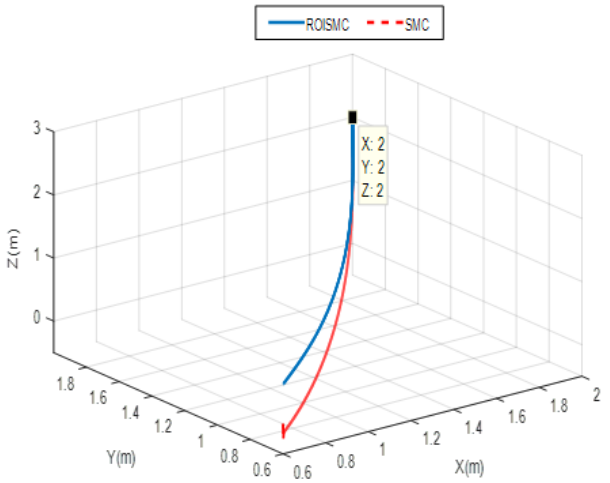


**Fig. 6** Global trajectory of the quadrotor position.

method, in this section a simulation is performed for a case that end-effector must track a predefined sinusoidal trajectory. The desired trajectory is a spiral which is described by a function of time. Thus, unlike the earlier part of the navigation path, the important thing for this simulation is to track the following trajectory by UAV sets:

$$x_d = 0.5\sin\left(\frac{2t+\pi}{2}\right), y_d = -0.5\sin\left(\frac{2t+\pi}{2}\right), z_d = -0.4\sin\left(\frac{4t+\pi}{2}\right)$$

In this section, the disturbances, including effects of unknown time varying wind disturbance, are considered in the close-loop system of the UAV according to (45). The position and attitude angle response of the system in the presence of wind field effect in predefined trajectory tracking are shown in Figs. 8 and 9. For the attitude angle the controller stabilized it at zero in a

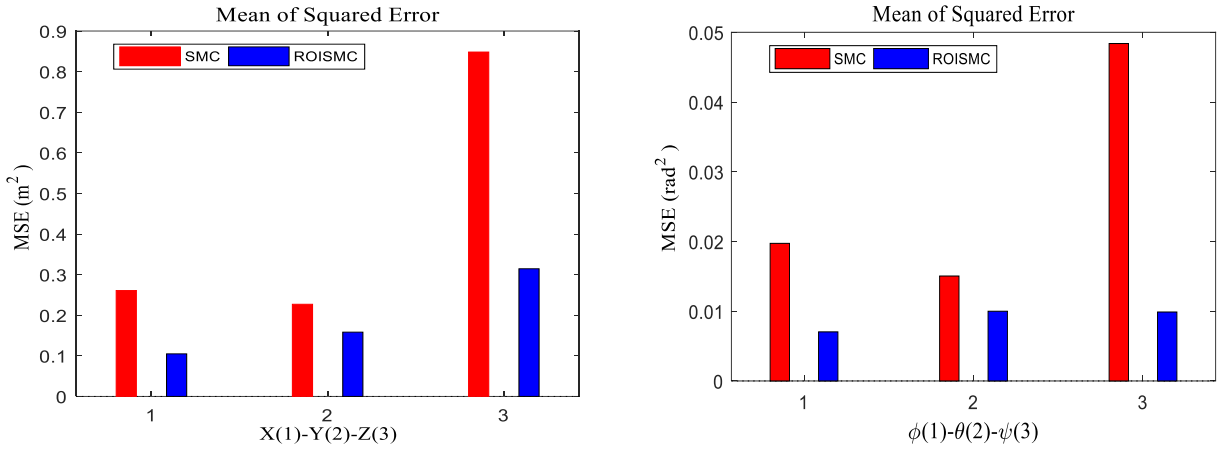


**Fig. 7** MSE quadrotor response comparison (SMC vs. ROISMC).

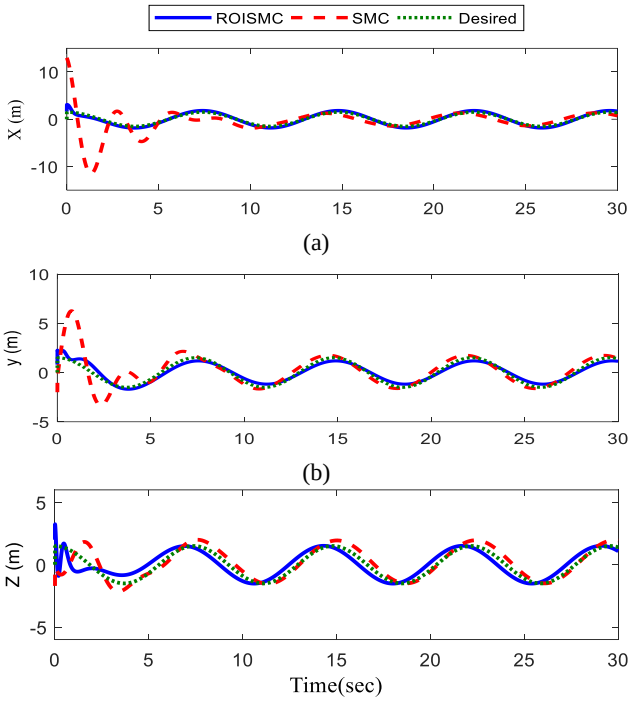


**Fig. 8** Tracking results of position ($x$, $y$, $z$).

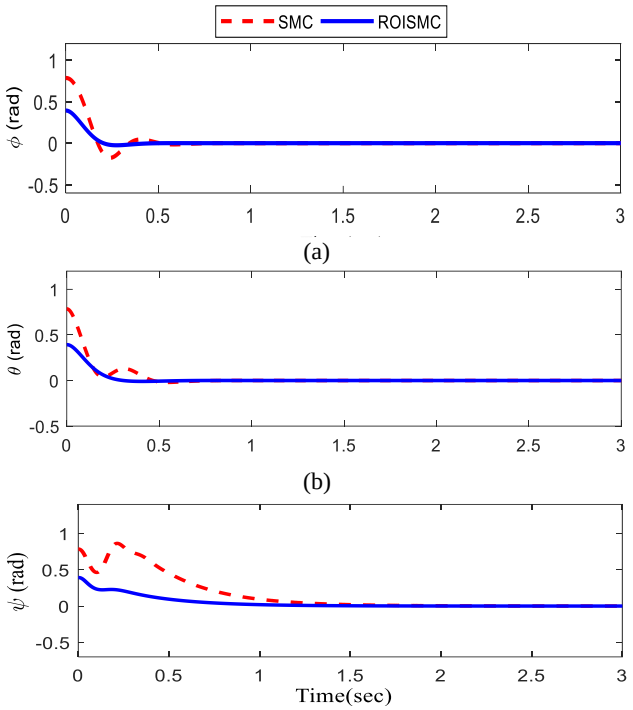


**Fig. 9** Tracking results of angle ($\varphi$, $\theta$, $\psi$).

short period of time. It can be seen that the control inputs are smooth and free of any chattering. The Convergence of position trajectories shown that even though the quadrotor position and attitude are affected by the abruptly changed reference positions and angles, the controller is able to drive all these state variables back to the new reference position and angle within seconds, as it can be seen in Fig. 8. They, exhibit the same behavior as the homologous positions and angles. Simultaneously, it is also shown that these state variables have coupling relationship, thus verifies the highly coupled characteristic of the dynamical model of the quadrotor. The controllers, displayed in Fig. 10, are continuous as desired and easily applied to a real-life model. It is noted that although the controllers reach their steady states several times during the flight process, the stability of them or the quadrotor does not appear affected. The control inputs are smooth and the chattering phenomena is decreased using the proposed controller. A comparison of the mean square error (MSE) for both SMC and ROISMC control is being presented in Fig. 11. Trajectory of a quadrotor in 3D space is also shown in Fig. 12.

### 5.3 Aggressive Maneuvers in Predefined Square Waveform Trajectory Tracking Under Time-Varying Wind Disturbances

In this experiment, the laboratory helicopter is required to achieve the position tracking for aggressive

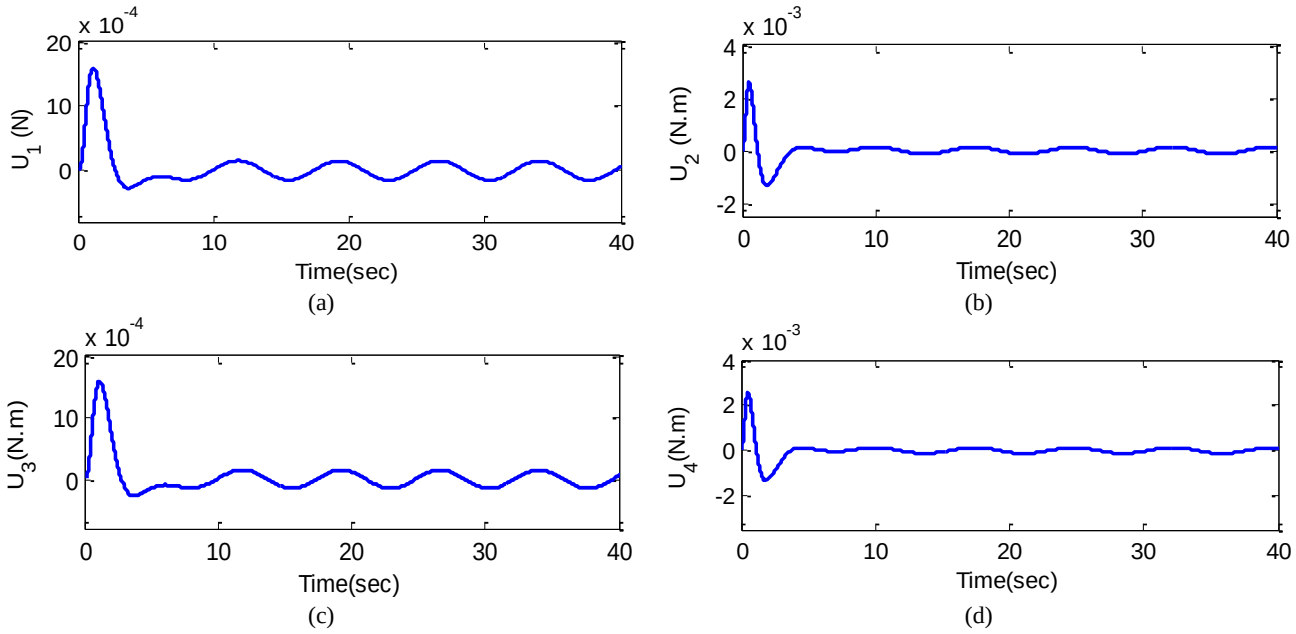


**Fig. 10** The output of the actuators.

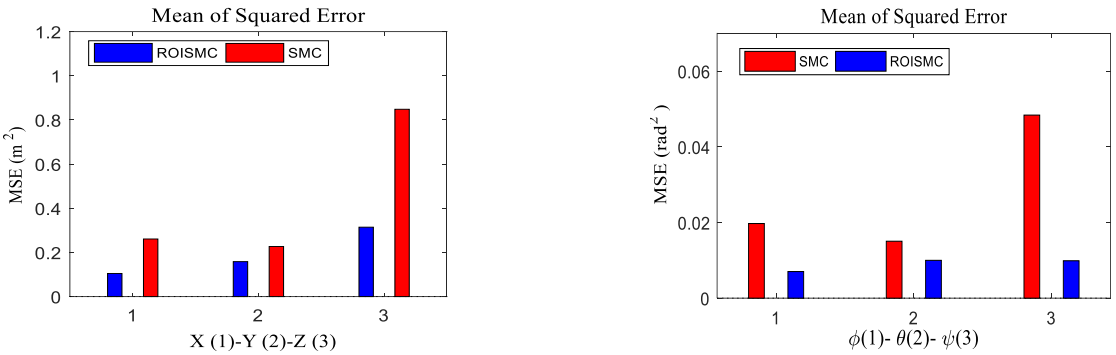


**Fig. 11** MSE quadrotor response comparison (SMC vs. ROISMC).

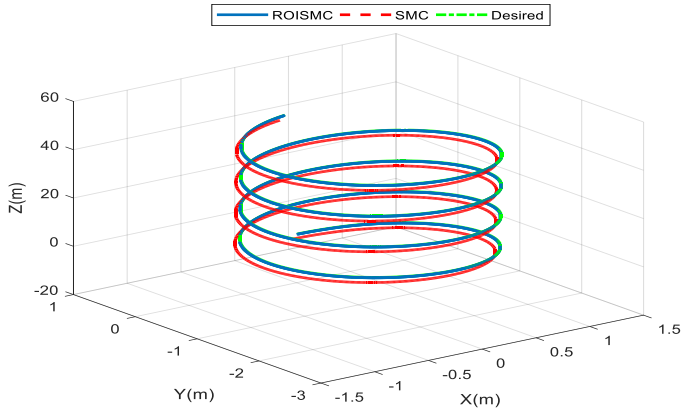


**Fig. 12** Global trajectory of the quadrotor position.

maneuvers under time-varying wind disturbances. The reference signals are given by

$$x_d = \left(\frac{1}{0.5s+1}\right)\overline{\omega_x}(s), y_d = \left(\frac{1}{2s+1}\right)\overline{\omega_y}(s), z_d = \left(\frac{1}{0.3s+1}\right)\overline{\omega_z}(s)$$

where $\overline{\omega_x}(s)$, $\overline{\omega_y}(s)$ and $\overline{\omega_z}(s)$ are the square waveform references with period (40-60 s).

Amplitudes are 0.8 radian and 2 m for the references of the attitude angles and position, respectively. This function is widely used in industrial applications. The unknown time varying wind disturbance in this section described in (45). When the aggressive maneuvers are

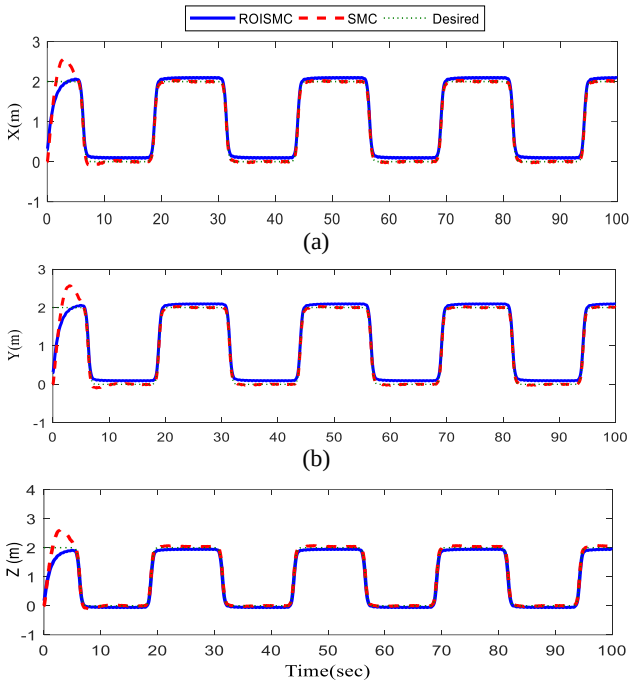


**Fig. 13** Tracking results of position ($x$, $y$, $z$).

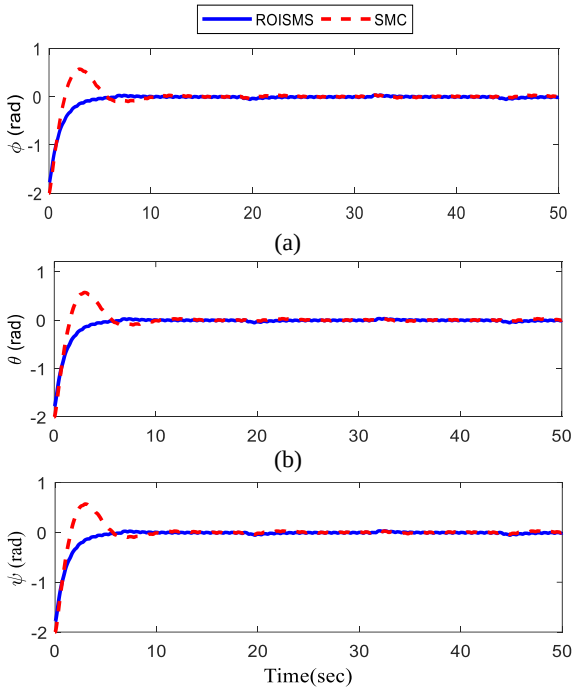


**Fig. 14** Tracking results of angle ($\varphi$, $\theta$, $\psi$).

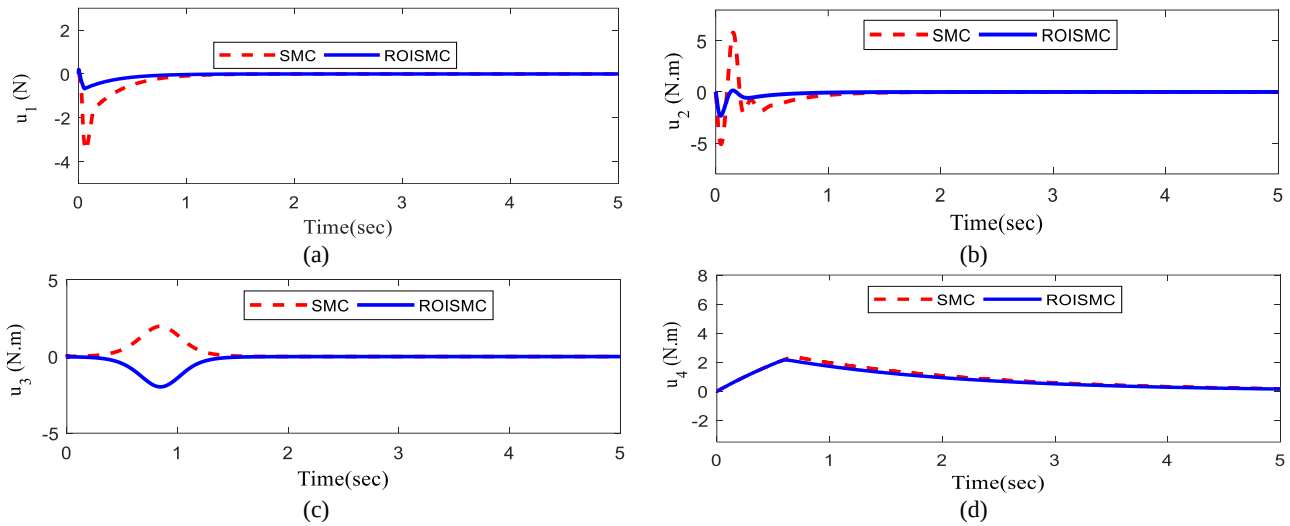


**Fig. 15** The output of the actuators.

implemented, one can see that the travel and elevation channels are affected by the additional forces produced by the wind gusts. The position and attitude angle response of the system in the presence of wind field effect and actuator faults in predefined waveform trajectory tracking are shown in Fig. 13 and 14, respectively. For the attitude angle the controller stabilized it at zero rad in a short period of time. It can be seen that the control inputs are smooth and free of any chattering. The Convergence of position trajectories stands for the quadrotor, according to the task, as it can be seen in Fig. 13. It is shown that even though the Quad rotor's position and attitude are affected by the abruptly changed reference positions and angles, the controller is able to drive all these state variables back to the new reference position and angle within seconds. It is obvious that the domain of effort control is significantly reduced which is the other benefit of the SDRE technique. The controllers, displayed in Fig. 15, are continuous as desired and easily applied to a real-life model. A comparison of the mean square error (MSE) for both SMC and ROISMC control is being presented in Fig. 16. In cases, given the large sampling period $1/T_s$ = 0.001 s, the ROISMC-controlled system has superior response, and still outperforms in comparison with the SMC control scheme when the sampling period decreases ($1/T_s$ = 0.1 s).

Those demonstrate the robustness of the designed

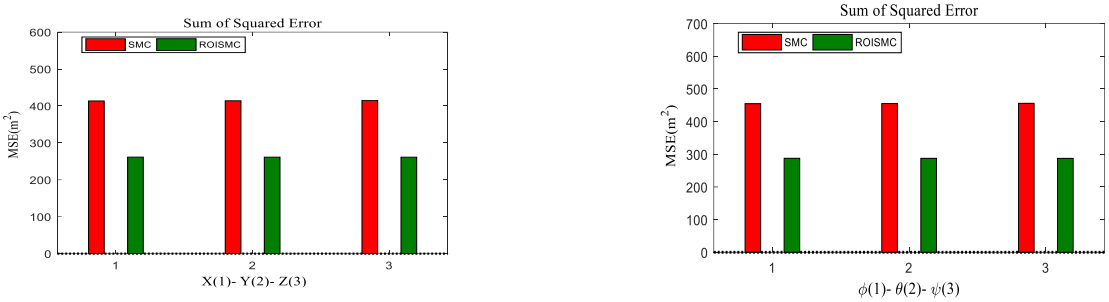


(a) (b)

**Fig. 16** MSE quadrotor response comparison (SMC vs. ROISMC).

**Table 1** Amount of cost function for two methods.

| | Cost Function | | |
|---|---|---|---|
| Algorithm | Set point | Sinusoidal | Square Wave Form |
| SMC | 334.34 | 428.36 | 412.75 |
| ROISMC | 275.53 | 396.42 | 384.27 |

controller and effectiveness of the proposed control scheme. Also, by comparing ROISMC method with the SMC approach, the optimality of the controller is checked in finding the best performance. The amounts of ROISMC and SMC cost function, for three cases are explained in Table 1.

It is obvious that the lowest amount of the cost function is for ROISMC method; therefore, the method suggested, has optimal performance rather than SMC approach. In summary, the results show that the proposed ROISMC controller accurately tracks the desired reference pulse, while providing fast and precise responses, and effectively attenuate the high speed wind. The small steady state error is being related to the wind's blowing direction and speed.

## 5 Conclusion

This paper presents a new technique developed based on SDRE and ISMC for UAV quadrotor systems. The optimal robust integral sliding mode control (ROISMC) was applied to address the position control for aggressive mission with actuators' faults and in presence of wind field effects. We first extracted the dynamic model for quadrotor using Newton-Euler formulation. The sliding surface of the proposed controller ensured the system robustness against the influences of actuators' faults. Then, the second method of Lyapunov theory was applied to guarantee the stability of the overall control system. An extensive numerical simulation was run to accredit the efficiency of proposed model and control scheme. Qualities of high accuracy, small position errors, optimal ranges of input control and minimum influence of the nonlinearities on the performance of UAV are other advantages of our proposed. Our future work focuses on developing more nonlinear control techniques (e.g. adaptive integral backstepping) with on-line fault detector in order to distinguish between external disturbance and actuator fault and finally fault tolerant control at the same time.

## References

[1] S. L. W. Gabriel, M. Hoffmann, and C. J. Tomlin, "Quadrotor helicopter trajectory tracking control," in *AIAA Guidance, Navigation and Control Conference*, South Carolina, Honolulu, Hawaii, Aug. 2008.

[2] S. Bouabdallah, A. Noth , and R. Siegwart, "PID vs LQ control techniques applied to an indoor micro quadrotor," in *IEEE International Conference on Intelligent Robots and Systems*, pp. 2451–2456, Oct. 2004.

[3] L. Wang, C. He, and P. Zhu, "Adaptive sliding mode control for quadrotor aerial robot with I type configuration," *International Journal of Automation and Control Engineering (IJACE)*, Vol. 3, pp. 20–26, 2014.

[4] V. T. Duong, H. Kyeong Kim, T. T. Nguyen, S. J. Oh, and S. B. Kim, "Position control of a Small scale quadrotor using block feedback linearization control," *Recent Advances in Electrical Engineering and Related Sciences Lecture Notes in Electrical Engineering*, Vol. 282,pp. 525–534, 2014.

[5] C. M. Lin, C. S. Hsueh, and C. H. Chen, "Robust adaptive backstepping control for a class of nonlinear systems using recurrent wavelet neural network," *Neurocomputing*, Vol. 142, pp. 372–382, 2014.

[6] B. Sumantri, N. Uchiyama, S. Sano, and Y. Kawabata, "Robust tracking control of a quad-rotor helicopter utilizing sliding mode control with a nonlinear sliding surface," *System Design and Dynamics*, Vol. 7,pp. 226–241, 2013.

[7] J. J. Xiong and E. H. Zheng, "Position and attitude tracking control for a quadrotor UAV," *ISA Transactions*, Vol. 53, No. 3, pp. 725–731, 2014.

[8] N. Jamali Soufi Amlashi, M. Rezaei, M. Bolandi, and A. Khaki Sedigh, "Robust second order sliding mode control for a quadrotor considering motor dynamics," *International Journal of Control Theory and Computer Modeling (IJCTCM)*, Vol. 4, No. 1/2 pp. 9–25, 2014.

[9] R. Avram, X. Zhang, and J. Muse, "Nonlinear adaptive fault-tolerant quadrotor altitude and attitude tracking with multiple actuator faults," *IEEE Transactions on Control Systems Technology*, Vol. 26, No. 2, pp. 701–707, 2018.

[10] E. B. Erdem and A. G. Alleyne, "Design of a class of nonlinear controllers via state dependent Riccati equations," *IEEE Transactions on Control Systems Technology*, Vol. 12, pp.133–137, 2004.

[11] C. P. Mracek, J. R. Cloutier," Control designs for the nonlinear benchmark problem via the state-dependent Riccati equation method," *International Journal of Robust and Nonlinear Control*, Vol. 4, pp. 401–433, 1998.

[12] T. D. Do, S. Kwak, H. H. Choi, and J. W. Jung, "Suboptimal control scheme design for interior permanent-magnet synchronous motors: An SDRE-based approach," *IEEE Transaction on Power Electronics*, Vol. 29, pp. 3020–3031, 2014.

[13] M. Massari and M. Zamaro, "Application of SDRE technique to orbital and attitude control of spacecraft formation flying," *Acta Astronautica*, Vol. 94, pp. 409–420, 2014.

[14] M. H. Korayem, A. Zehfroosh, H. Tourajizadeh, and S. Manteghi, "Optimal motion planning of non-linear dynamic systems in the presence of obstacles and moving boundaries using SDRE: Application on cable-suspended robot," *Nonlinear Dynamic*, Vol. 76, pp. 1423–1441, 2014.

[15] M. Abdelrahman, I. Chang, and S. Park, "Magnetic torque attitude control of a satellite using the state-dependent Riccati equation technique," *International Journal of Non-Linear Mechanics*, Vol. 46, pp. 758–771, 2011.

[16] Y. Zhang, S. Agrawal, P. Hemanshu, and M. Piovoso, "Optimal control using State Dependent Riccati equation (SDRE) for a flexible cable transporter system with arbitrarily varying lengths," in *Proceedings of IEEE Conference on Control Applications*, Canada, pp. 1063–1068, 2005.

[17] K. Runcharoon and V. Srichatrapimuk, "Sliding mode control of quadrotor," in: *International Conference of Technological Advances in Electrical, Electronics and Computer Engineering*, Konya, pp. 552–557, May 2013.

[18] Y. J. Huang, T. C. Kuo, and H. K. Way, "Robust vertical takeoff and landing aircraft control via integral sliding mode," in *IEE Proceedings-Control Theory and Applications*, Vol. 150, pp. 383–388, 2003.

[19] R. Babaie and A. F. Ehyaie, "Robust optimal motion planning approach to cooperative grasping and transporting using multiple UAVs based on SDRE," *Transactions of the Institute of Measurement and Control*, Apr. 2016.

[20] C. M. R. Oliveira, M. L. Aguiar, J. R. B. A. Monteiro, W. C. A. Pereira, G. T. Paula, and T. E. P. Almeida, "Vector control of induction motor using an integral sliding mode controller with anti-windup," *Journal of Control Automation & Electrical Systems*, Vol. 27, No. 2, pp. 169–178, 2016.

[21] X. Li and J. Zhou, "A sliding mode control design for mismatched uncertain systems based on states transformation scheme and chattering alleviating scheme," *Transactions of the Institute of Measurement and Control*, Vol. 40, No. 8, pp. 2509–2516, 2017.

[22] Y. Liu and Y. Niu "Sliding mode control for uncertain switched systems subject to state and input delays" *Transactions of the Institute of Measurement and Control*, Vol. 40, No. 10, pp. 3232–3238, 2017.

[23] I. González-Hernández, S. Salazar, A. E. Rodríguez-Mata, F. Muñoz Palacios, R. López, and R. Lozano, "Enhanced robust altitude controller via integral sliding modes approach for a quad-rotor aircraft: Simulations and real-time results," Journal of Intelligent & Robotic Systems, Vol. 88, No. 2–4, pp. 313–327, 2017.

[24] M. Chipofya and D. J. Lee, "Position and altitude control of a quadcopter using state-dependent Riccati equation (SDRE) control," in *17th International Conference on Control, Automation and Systems (ICCAS)*, Jeju, South Korea, 18-21 Oct. 2017.

[25] A. H. Korayem, S. R. Nekoo, and M. H. Korayem, "Sliding mode control design based on the state-dependent Riccati equation: Theoretical and experimental implementation," *International Journal of Control*, pp. 1–14, 2018.

[26] M. Li1, Z. Zuo1, H. Liu, C. Liu, and B. Zhu, "Adaptive fault tolerant control for trajectory tracking of a quadrotor helicopter," *Transactions of the Institute of Measurement and Control*, Vol. 40, No. 12, pp. 3560–3569, 2018.

[27] D. G. Luenberger, "Observing the state of a linear system", *IEEE Transactions on Military Electronics*, Vol. 8, No. 2, pp. 74–80, Apr. 1964.

[28] R. Babaie, A. F. Ehyaei, "Robust control design of a quadrotor UAV based on incremental hierarchical sliding mode approach," in *25th Iranian Conference on Electrical Engineering (ICEE2017)*, May 2017.

**R. Babaie** received her B.Sc. degrees in Electrical Engineering from Karaj Azad University, Karaj, Iran, in 2011 and the M.Sc. degree in Electrical Engineering from Imam Khomeini International University (IKIU), Qazvin, Iran, in 2015. Her research interests include nonlinear control systems, fault tolerant control system, robust control, optimization and robotics.

**A. F. Ehyaei** received his B.Sc. degree in Electrical Engineering from Sharif University of Technology, Tehran, Iran, in 2001 and M.Sc. and the Ph.D. degrees in Electrical Engineering from the Iran University of Science and Technology (IUST), Tehran, Iran, in 2003 and 2011, respectively. He is an Assistant Professor in the Electrical Engineering Department of Imam Khomeini International University since 2011. Also, he collaborates as a consultant with several companies in the field of instrumentation and process control. His main research activities include navigation and control of robotic systems, multi-agent systems, process control and automation.

© 2019 by the authors. Licensee IUST, Tehran, Iran. This article is an open access article distributed under the terms and conditions of the Creative Commons Attribution-NonCommercial 4.0 International (CC BY-NC 4.0) license (https://creativecommons.org/licenses/by-nc/4.0/).